Title

Ultrasound-Based Quantification of Vitreous Floaters Correlates with Contrast Sensitivity and Quality of LifeQUS Correlates with CS and VFQ

Journal

Investigative Ophthalmology & Visual Science, 56(3)

ISSN

0146-0404

Authors

Mamou, Jonathan
Wa, Christianne A
Yee, Kenneth MP
et al.

Publication Date

2015-03-05

DOI

10.1167/iovs.14-15414

Peer reviewed

Ultrasound-Based Quantification of Vitreous Floaters Correlates with Contrast Sensitivity and Quality of Life

Jonathan Mamou,[1] Christianne A. Wa,[2,3] Kenneth M. P. Yee,[2,3] Ronald H. Silverman,[1,4] Jeffrey A. Ketterling,[1] Alfredo A. Sadun,[3] and J. Sebag[2]

[1]F. L. Lizzi Center for Biomedical Engineering, Riverside Research, New York, New York, United States
[2]VMR Institute for Vitreous Macula Retina, Huntington Beach, California, United States
[3]Doheny Eye Institute/UCLA, Los Angeles, California, United States
[4]Department of Ophthalmology, Columbia College of Physicians & Surgeons, New York, New York, United States

Correspondence: J. Sebag, VMR Institute for Vitreous Macula Retina, 7677 Center Avenue, Suite 400, Huntington Beach, CA 92647, USA; jsebag@VMRinstitute.com.

Submitted: August 6, 2014
Accepted: January 7, 2015

Citation: Mamou J, Wa CA, Yee KMP, et al. Ultrasound-based quantification of vitreous floaters correlates with contrast sensitivity and quality of life. *Invest Ophthalmol Vis Sci*. 2015;56:1611–1617. DOI:10.1167/iovs.14-15414

Purpose. Clinical evaluation of floaters lacks quantitative assessment of vitreous structure. This study used quantitative ultrasound (QUS) to measure vitreous opacities. Since floaters reduce contrast sensitivity (CS) and quality of life (Visual Function Questionnaire [VFQ]), it is hypothesized that QUS will correlate with CS and VFQ in patients with floaters.

Methods. Twenty-two eyes (22 subjects; age = 57 ± 19 years) with floaters were evaluated with Freiburg acuity contrast testing (FrACT; %Weber) and VFQ. Ultrasonography used a customized probe (15-MHz center frequency, 20-mm focal length, 7-mm aperture) with longitudinal and transverse scans taken in primary gaze and a horizontal longitudinal scan through premacular vitreous in temporal gaze. Each scan set had 100 frames of log-compressed envelope data. Within each frame, two regions of interest (ROIs) were analyzed (whole-central and posterior vitreous) to yield three parameters (energy, E; mean amplitude, M; and percentage of vitreous filled by echodensities, P50) averaged over the entire 100-frame dataset. Statistical analyses evaluated E, M, and P50 correlations with CS and VFQ.

Results. Contrast sensitivity ranged from 1.19%W (normal) to 5.59%W. All QUS parameters in two scan positions within the whole-central ROI correlated with CS ($R > 0.67$, $P < 0.001$). P50 in the nasal longitudinal position had $R = 0.867$ ($P < 0.001$). Correlations with VFQ ranged from $R = 0.52$ ($P < 0.013$) to $R = 0.65$ ($P < 0.001$).

Conclusions. Quantitative ultrasound provides quantitative measures of vitreous echodensity that correlate with CS and VFQ, providing objective assessment of vitreous structure underlying the functional disturbances induced by floaters, useful to quantify vitreous disease severity and the response to therapy.

Keywords: vitreous, ultrasonography, contrast sensitivity, quality of life, floaters

The vitreous body is normally a homogeneous, optically, and acoustically transparent gel filling the posterior segment of the eye.[1,2] The volume of gel vitreous increases during the first decade of life while the eye is growing in size and then remains stable until about the age of 40 years, when it begins to decrease in parallel with an increase in liquid vitreous. Macromolecular changes in collagen-hyaluronan interaction during the process of liquefaction result in structural inhomogeneities throughout the vitreous body.[3] Conditions such as diabetes[4–7] and myopia[8] accelerate vitreous liquefaction and the formation of intravitreal collagen aggregates, which cause light scattering and can induce the clinical phenomenon of floaters.[4,8,9]

Concurrently, changes due to aging at the vitreoretinal interface promote decreased adhesion of the posterior vitreous cortex to the inner limiting membrane (ILM) of the retina.[10–12] The factors that promote weakening of vitreoretinal adhesion are not well understood, but probably result from alteration of the various extracellular matrix molecules found at the vitreoretinal interface.[13,14]

When vitreous liquefaction and vitreoretinal dehiscence develop in concert, the eventual result is separation of the posterior vitreous cortex from the ILM, a condition known as posterior vitreous detachment (PVD). The dense collagen matrix of the posterior vitreous cortex that is displaced anterior to the retina during PVD often scatters light sufficiently to interfere with photon transmission casting shadows on the retina that are perceived as hair-like, gray linear structures. Posterior vitreous detachment is the most common cause of floaters.[2,9,15]

Although quite prevalent, floaters have historically not been considered a significant problem meriting therapeutic intervention.[16] This is partly because the diagnosis of floaters is largely based on subjective patient self-evaluation and in most cases floaters do not substantially reduce visual acuity. Nonetheless, for some individuals, floaters cause serious degradation in the quality of life.[17,18] What has been lacking is a better understanding of why floaters cause such unhappiness, as well as reproducible, objective clinical measures of floater severity.

Recent studies[19] have determined that floaters degrade contrast sensitivity (CS) by an average of 67%. While CS measurements do evaluate the impact of floaters on vision better than visual acuity,[9] the test involves patient input with

attendant limitations such as patient comprehension and compliance, making CS subjective to some degree. Contrast sensitivity is also influenced by corneal irregularities,[20–22] lens opacification,[23,24] and multifocal intraocular lenses,[25,26] further limiting its utility. A more objective way to assess vitreous floaters is thus needed. In particular, objective, quantitative measures of the structural changes that cause floaters are lacking from the clinical evaluation of this condition.

Optical coherence tomography (OCT) permits visualization of abnormalities at the vitreoretinal interface, but does not permit adequate imaging of the entire vitreous body. In contrast, ultrasound, which is sensitive to microscale (on the order of 40 μm at 15 MHz) tissue alterations related to changes in mass density (e.g., liquefied versus gel vitreous) and particle size and particle concentration (e.g., vitreous collagen aggregation), permits visualization of the entire vitreous body. Thus, standard ultrasound images (B-mode) are representations of microstructure variations in the acoustic impedance (density X speed-of-sound) of vitreous. The images are usually qualitative, but quantitative ultrasound (QUS) methods have been developed to process raw, phase-resolved, radio-frequency (RF) backscatter data in a system- and user-independent fashion in order to derive a quantitative assessment of acoustic tissue properties.[27] Quantitative ultrasound methods have been successfully applied to the detection of ocular tumors,[28] lymph nodes cancers,[29] and various other diseases and tissues.[30] Although video represents a reduced set of information relative to the raw RF, B-mode video data may still be analyzed using QUS methods.[27,31,32]

The aim of the present study was to develop QUS methods to quantify vitreous inhomogeneities in patients with floaters and to determine if these QUS measures of structural vitreous densities correlate with functional deficits in vision, particularly CS, as well as the level of patient dissatisfaction with vision. It was hypothesized that QUS measures of the degree of vitreous inhomogeneity will correlate with CS values as well as the National Eye Institute (NEI) Visual Function Questionnaire (VFQ) assessment of visual function and quality of life.

Materials and Methods

Subjects

All study protocals were IRB approved. No subjects with a history of vitreoretinal surgery, diabetes, intravitreal injections, or laser photocoagulation therapy were included. Twenty-two eyes from 22 subjects (11 men and 11 women) were evaluated. The average age was 57 ± 19 years. Eighteen eyes were phakic and four were pseudophakic, none with multifocal intraocular lenses. All patients had floaters in both eyes, but in the majority (17/22; 77%) one eye was subjectively worse and was selected for this study. In 5 of 22 (23%) of subjects, both eyes were comparably affected, and thus one eye was randomly chosen for study inclusion.

The etiology of floaters was PVD in 14 of 22 (63.6%), and myopic vitreopathy in 3 of 22 (13.6%) eyes, consistent with previous studies.[19] Three eyes had retinal cryopexy to treat retinal breaks at least 3 months prior to study entry. In addition, three other eyes had undergone neodymium-doped yttrium aluminum garnet (YAG) laser treatments for floaters at least 12 months prior to study inclusion.

To evaluate subjective well-being, the NEI validated VFQ was completed by each patient on the same visit as ultrasonography. A composite score consisting of six of the standard VFQ subsections relating to visual function (general vision, near activities, distance activities, driving, color vision, and peripheral vision) was calculated.

Contrast Sensitivity Measurements

Contrast sensitivity was measured using computer-based Freiburg Acuity Contrast Testing (FrACT).[19,33–35] This test was developed at the University of Freiburg in Germany and is freely available online in the public domain at http://www.michaelbach.de/fract/index. The exact same test has previously been used in the exact same way to measure CS in patients with floaters.[19] FrACT is based on a gapped Landolt ring stimulus (i.e., a "tumbling C") that is presented as a gray symbol on a lighter background in one of eight possible positions. The test uses best parameter estimation by sequential testing (PEST) adaptive threshold estimation to adjust the difficulty of the task across trials according to the subject's performance. All subjects were dark adapted for 3 minutes and then tested at a distance of 2.9 m in a dark room. Vision was corrected if the patient was ametropic. The testing software reports the CSF value in terms of the Weber index:

$$\%W = \frac{Luminance_{max} - Luminance_{min}}{Luminance_{max}}. \quad (1)$$

Contrast sensitivity testing was not done under photopic or scotopic conditions because mesopic vision is a combination of photopic and scotopic vision in low but not quite dark light settings at luminance levels range from 0.01 to 1 cd m. Therefore, this was the fairest measure of what patients would usually experience. In addition, the fact that CS was highly correlated with VFQ scores (see below) suggests that the patient's reality was well-captured.

Ultrasonography

Instrumentation. A customized high-frequency ultrasound system (Aviso; Quantel Medical, Clermont-Ferrand, France) was used at the VMR Institute for Vitreous Macula Retina (Huntington Beach, CA, USA). This system employed a single-element, focused transducer operating at a 15-MHz center frequency with a 6-dB bandwidth extending from 9.5 to 20.0 MHz. The focal length of the transducer and the aperture were 20 and 7 mm, respectively. The system was customized to provide the log-compressed envelope data, sampled at 40 MHz, before scan conversion and video display. The envelope data were obtained by Hilbert transform, which is equivalent to demodulating the RF data by the center frequency of the transducer. Therefore, the demodulated signal has much lower bandwidth and can be sampled at lower rates.

Data Acquisition. After visual acuity measurement and contrast sensitivity testing, topical anesthesia was induced with proparacaine 2% and Systane gel (0.3% hypromellose; Alcon, Inc., Fort Worth, TX, USA) was applied to the tip of the ultrasound probe. The probe was placed directly on the globe to avoid ultrasound attenuation by the eyelid. The contact point with the globe was behind the limbus to avoid signal attenuation by the lens. Ultrasonography was performed in three scan orientations for each eye. With the patient in primary gaze, the probe was placed on the inferotemporal aspect of the globe posterior to the limbus. A longitudinal scan and a transverse scan approximately through the plane of the macula were acquired. These two scan orientations will be referred to as LONG and TRANS, respectively. With the patient gazing temporally, and the probe on the nasal aspect of the globe posterior to the limbus, a horizontal longitudinal scan was acquired through the plane of the macula (referred to as LMAC).

The ultrasound settings were standardized for all measurements: 100 total frames acquired at 16 frames/second, 40-mm image depth, 50° sector scan, and 1024 × 170 image resolution. All ultrasound system settings were kept constant for each

Investigative Ophthalmology & Visual Science

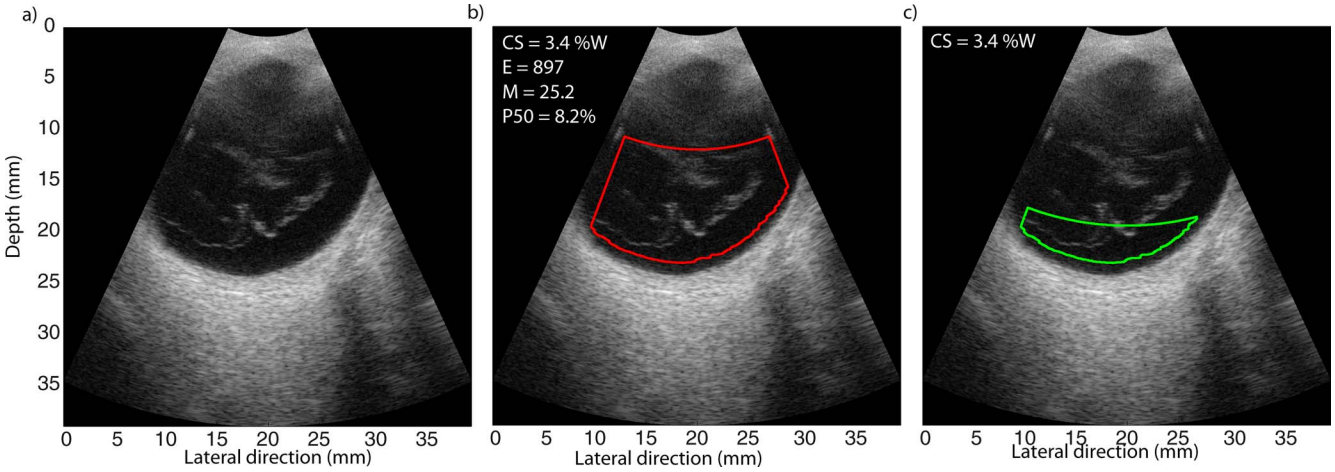

Figure 1. (**a**) Illustrative ultrasound image of an eye with visible echodensities. (**b**) Whole-central vitreous ROI outlined in *red*. (**c**) Posterior vitreous ROI outlined in *green*.

subject to allow for direct and quantitative comparison of the images. In particular, the gain and contrast were always set to 105 and 80 dB, respectively.

Quantitative Ultrasound Data Processing

The acquired raw ultrasound data were transferred from VMR Institute to Riverside Research and processed offline to calculate QUS parameters. Quantitative ultrasound processing was performed using automatic algorithms developed in Matlab (The Mathworks, Natick, MA, USA). Each data set from each eye and each position contained 100 B-mode images acquired at 16 frames/sec. Image stacks were individually inspected and only artifact-free frames were processed. Within each artifact-free frame, two distinct regions of interest (ROIs) were automatically selected. The first ROI included the entire vitreous considered to be within the depth of field of the ultrasound image. The second ROI was smaller and entirely included within the first ROI. These two ROIs were termed whole-central vitreous ROI and posterior vitreous ROI, respectively (Figs. 1, 2).

In each artifact-free frame, ROIs were automatically found by using an edge detection algorithm to find the retinal surface and cutting off A-lines on each edge of the B-mode image. The whole-central vitreous ROI was started at a distance of 11.7 mm (from the ultrasound transducer) because the ultrasound image was not in focus anterior to that position. The posterior ROI was started at a depth of 19.5 mm because it was approximately 4 mm in front of the macula. The rationale behind the delineation of the whole-central vitreous ROI was to include as much of the vitreous body as possible for any given eye in the QUS evaluation. Therefore, this ROI begins at the depth at which the image quality was sufficient (i.e., the beginning of the focal region of the transducer) and extends to within 1 mm of the retinal surface. In the case of the posterior ROI, the anterior boundary was fixed at 19.5 mm from the transducer, producing an ROI approximately 4 mm in axial depth. Because the algorithm adapted to the orientation of the eye and scan plane, there was some variation from scan to scan, but the same ROI was always produced for the same scan. Figure 1a shows an illustrative ultrasound image and the two ROIs are outlined in Figures 1b and 1c.

Each ROI was processed to yield three distinct QUS parameters: energy (*E*), mean (*M*), and the percentage of the ROI filled by floaters (*P*50). The rationale behind the choice of these three QUS measures was that normal vitreous typically has low echodensity, which should yield low values for all

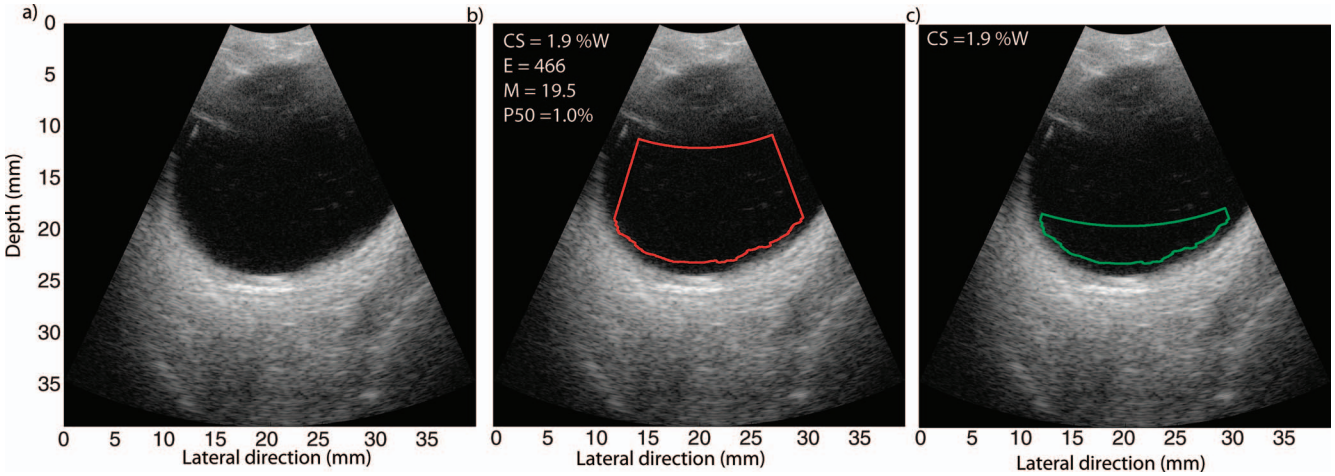

Figure 2. (**a**) Illustrative ultrasound image of an eye with no visible echodensities. (**b**) Whole-central vitreous ROI outlined in *red*. (**c**) Posterior vitreous ROI outlined in *green*.

Investigative Ophthalmology & Visual Science

Table 1. Reproducibility of Quantitative Ultrasound (QUS)

	Energy			Mean			P50		
ROI	LMAC	LONG	TRANS	LMAC	LONG	TRANS	LMAC	LONG	TRANS
Whole	0.923	0.855	0.275	0.892	0.828	0.325	0.903	0.860	0.326
Posterior	0.319	0.663	0.340	0.371	0.644	0.313	0.247	0.742	0.646

Reproducibility was assessed using intraclass correlation (rICC) analyses on a cohort of 10 eyes in 10 subjects for which ultrasound data was collected and processed to yield QUS indices three separate times.

these QUS parameters, whereas floaters are echogenic, which should yield increased values of QUS parameters. Energy was defined as the sum of the square of the acoustic values within the ROI divided by the ROI area. The acoustic values were defined as the digitized envelope values between 0 and 255. Mean was defined as the mean of the acoustic values divided by the ROI size. *P*50 was obtained by computing the percentage of the ROI filled by clusters of echogenic regions greater in size than 50 pixels (i.e., 0.069 mm). This size was chosen after inspecting the images and noting that most vitreous opacities were at least that size or bigger and that smaller echogenic regions typically were associated with noise. In a last step, the QUS parameters were averaged over the number of artifact-free frames. Similarly, *P*25 and *P*75 were also investigated, but results were nearly identical to those obtained with *P*50 and are therefore not reported. To depict how the QUS methods work, two illustrative images were chosen because they are representative of the 22-eye cohort included in this study. Figure 1 is representative of an eye with a large amount of echodensities and Figure 2 is representative of an eye with minimal echodensities.

Reproducibility

To determine the reproducibility of QUS measurements, 10 eyes from 10 additional subjects (5 men and 5 women; mean age = 65.7 ± 12.2 years) with some degree of subjective vitreous floaters were scanned three times on the same day. Each scan orientation was imaged three times sequentially by the same operator. Reproducibility was quantified by computing the intraclass correlation for each QUS estimate, each scan orientation, and both ROIs. Reproducibility was judged satisfactory if the correlation coefficient exceeded 0.80.

Statistical Analyses

Statistical analyses were conducted to assess whether the QUS indices correlated with CS or VFQ scores. To this end, Spearman (ρ) correlations and associated *P* values were computed between each QUS parameter and CS value or VFQ score for each eye, scan position, and ROI. Spearman correlations were computed because some of the investigated QUS parameters failed the Kolmogorov-Smirnov (K-S) test for normal distribution (i.e., associated *P* values < 0.05). Spearman correlations were deemed significant if the associated *P* value was smaller than 0.05. For this study, each eye was treated as independent (i.e., each eye was independently evaluated for CS and VFQ).

Results

Reproducibility

The intraclass correlation results (Table 1) show that satisfactory reproducibility ($R \geq 0.828$) was obtained from all three QUS indices in the whole-central ROI in the LMAC and LONG scanning orientations. In contrast, all results obtained in the TRANS orientation or in the posterior ROI showed suboptimal reproducibility; *R* less than or equal to 0.326 and *R* less than or equal to 0.742, respectively. Thus, results obtained in the TRANS scan orientation and all measurements from the posterior ROI in the 22-eye cohort will not be presented below.

Contrast Sensitivity (CS)

The CS measured in 22 eyes from 22 patients with vitreous floaters ranged from 1.19 %W (normal) to 5.59 %W (worst). The average CS was 2.93 ± 1.27 %W, consistent with previously published data[19] where control subjects had an average of 2.4 %W, while patients complaining of clinically significant floaters had an average of 4.0 %W ($P < 0.01$). Figure 3 illustrates that CS was inversely and significantly correlated with the composite score of six VFQ indices (not normally distributed by K-S test) with Spearman correlation = –0.765 and $P < 0.001$, meaning that the worse the CS the more dissatisfaction with vision.

Quantitative Ultrasound (QUS) Parameters From Illustrative Eyes

Figures 1b and 2b show the CS values and QUS parameters for the whole-central vitreous ROIs for the two representative eyes described above. As expected, *E*, *M*, and *P*50 were larger for the eye with visible floaters. The representative examples of floaters versus no floaters in these figures indicate that all QUS indices increase when the ROI contains punctate and linear vitreous echodensities. (Note: QUS indices are not reported for

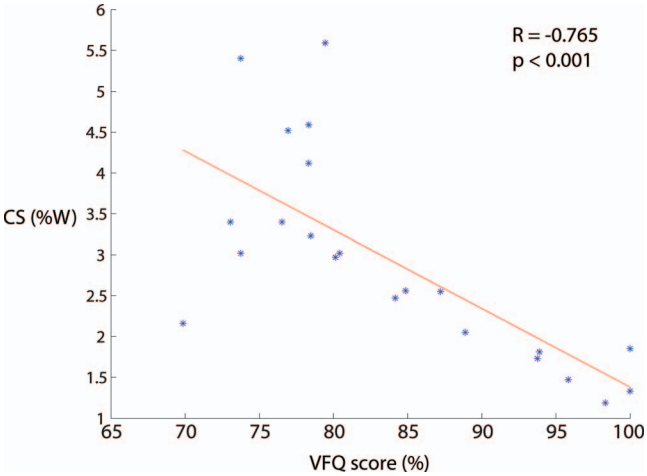

Figure 3. Correlation of CS with VQF. There is a strong correlation between decreasing levels of patient satisfaction with vision (lower VFQ score on *x*-axis) with degradation of contrast sensitivity (CS; higher Weber Index on *y*-axis).

Table 2. Correlation of Quantitative Ultrasound (QUS) With Contrast Sensitivity

	Energy		Mean		P50	
	LMAC	LONG	LMAC	LONG	LMAC	LONG
Whole ROI *R*	0.827	0.734	0.801	0.739	0.867	0.669
Whole ROI *P*	<0.001	<0.001	<0.001	<0.001	<0.001	0.001

Spearman correlation (*R*) and associated *P* values between contrast sensitivity and reproducible quantitative ultrasound indices (LMAC and LONG in the whole vitreous ROI) showed a positive correlation with increased QUS indices (increased vitreous echodensity) being strongly correlated with worse contrast sensitivity (increased Weber index).

the posterior ROI because of the results of the reproducibility study.)

Correlation of QUS With CS

Table 2 displays the Spearman correlations (*R*) and associated *P* values for each QUS parameter, scan orientation, and ROI as compared with CS. As indicated above, only the reproducible analyses are presented. The results show that all correlations were significant, with *R* varying between 0.867 and 0.669. The best correlation ($R = 0.867$) was obtained for *P*50 in the LMAC scan orientation and a slightly lower value ($R = 0.734$) was obtained for *E* in the LONG orientation. Table 2 also reveals that *P*50 seems to be less informative than *E* and *M* in the LONG orientation.

Figure 4 shows scatter plots with best-fit linear regressions for the correlations between QUS and CS for three ultrasound scan parameters. Figure 4a shows the values for *E* obtained in the LMAC position ($R = 0.849$ and $P < 0.001$), with a good linear fit and no visible outliers. Figure 4b shows slightly lower correlation ($R = 0.776$) obtained for *M* in the LONG orientation. This plot also reveals a good linear fit except for the eye with the largest CS value (5.59%W). Removing this outlier did not significantly affect *R* and *P* values (*R* became 0.700 with $P < 0.001$). Finally, Figure 4c shows the best correlation (i.e., $R = 0.867$) obtained for *P*50 in the LMAC scan orientation. As expected, a good linear fit is evident.

Correlation of QUS With VFQ

Table 3 displays the correlations obtained when comparing QUS indices to VFQ scores. All QUS parameters were negatively and significantly correlated with VFQ scores, meaning the greater the QUS measure of vitreous echodensity, the more dissatisfaction with vision. The absolute *R* values range between 0.521 and 0.651.

Figure 5 shows scatter plots with best-fit linear regressions for three scan orientations in all study eyes shown in Table 3. For comparison purposes, the three scan orientations are the same as those shown in Figure 4. As expected because of the lower absolute *R* values, Figure 5 illustrates that there is more variability around the linear regressions than in Figure 4. Even though CS and VFQ were reasonably well correlated with each other (Fig. 3), the results shown in Tables 2 and 3 reveal that QUS indices would provide more objective and better quantitative criteria to assess the severity of the condition.

Discussion

This study was undertaken to develop QUS as an objective index of vitreous echodensity in a clinical setting. The

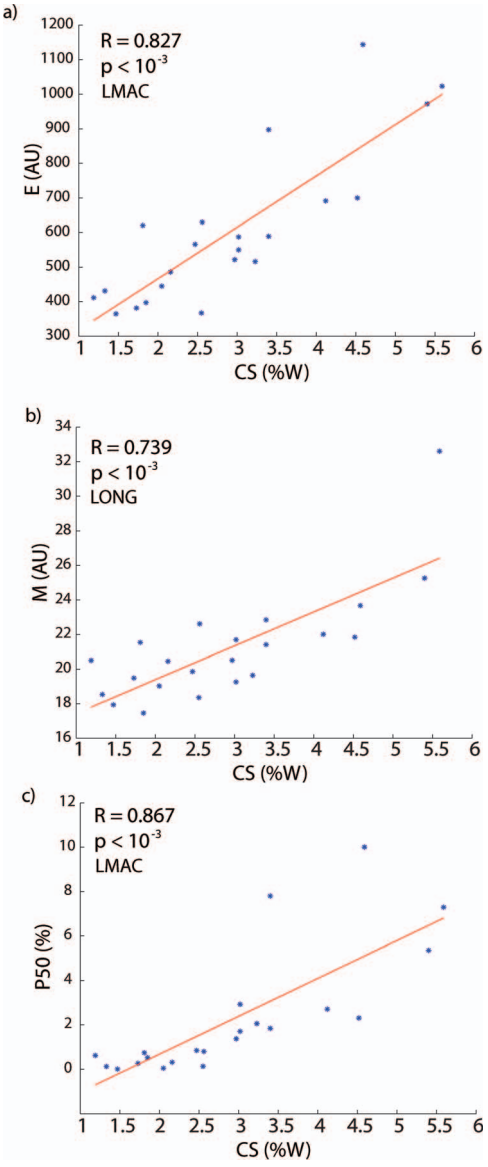

Figure 4. Correlations between QUS (arbitrary units, AU) and CS (%W) in different ultrasound scan orientations. (**a**) Whole-central *E* index from LMAC data, (**b**) whole-central *M* index from LONG data, and (**c**) whole-central *P*50 index from LMAC data. (Removing the outlier point in [**b**] did not significantly affect results, as *R* became 0.700 with $P < 0.001$.)

results were compared to the NEI VFQ and to CS. Contrast sensitivity is a visual function that has been shown to diminish in patients with floaters, yet was normalized within 1 week of limited vitrectomy in every case tested to date.[19] The results presented herein indicate that QUS measures reflect a range of vitreous echodensities and that these parameters correlate positively with the degradation in CS as well as the patient dissatisfaction index quantified by VFQ measures. Indeed, the best correlation between QUS and CS ($R = 0.867$, $P < 0.001$) is very encouraging and provides a rationale for continued development of QUS imaging protocols and quantitative analyses to provide enhanced clinical assessment of the severity of floaters and vitreous structure in this and other clinical conditions.

The QUS parameters computed in this study could be directly compared between eyes because the settings on the

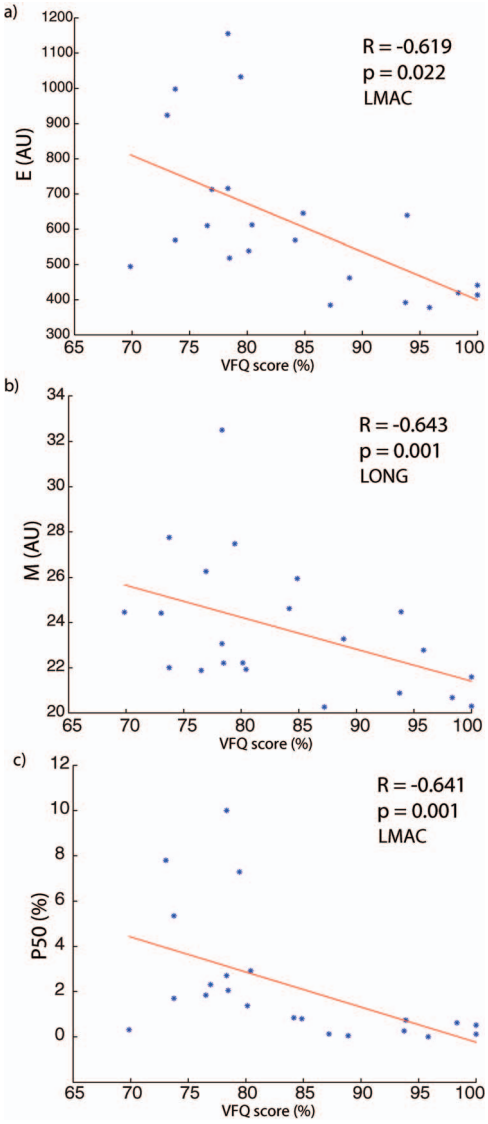

Figure 5. Correlations between QUS in different scan orientations and VFQ assessment of patient dissatisfaction with vision. (**a**) Whole-central *E* index from LMAC data, (**b**) whole-central *M* index from LONG data, and (**c**) whole-central *P*50 index from LMAC data. The greater the QUS indices, the lower patient satisfaction with vision (VFQ).

ultrasound scanner were kept constant for all measurements. It should be noted, however, that these indices were obtained from the log-compressed envelope signal, which is suboptimal from a signal-processing perspective. Ideally, the QUS approach should be applied to the raw, phase-resolved backscatter echo signal, which contains more information about underlying tissue structure. Thus, new QUS methods based on the phase-resolved data are being developed and evaluated, with the anticipation that this will improve the sensitivity of this quantitative diagnostic approach. In fact, one such QUS parameter related to the effective scatterer size can be used to assess the size of the underlying vitreous macromolecules responsible for ultrasound scattering.[27] This QUS parameter has been shown to reliably detect cancerous regions in the human lymph node[31,36] and based on the study presented herein holds promise for structural assessment of vitreous in vivo.

Table 3. Correlation of Quantitative Ultrasound (QUS) with Patient Vision Dissatisfaction as Quantified by NEI Visual Function Questionnaire (VFQ)

	Energy		Mean		P50	
	LMAC	LONG	LMAC	LONG	LMAC	LONG
Whole ROI *R*	−0.619	−0.651	−0.651	−0.643	−0.641	−0.521
Whole ROI *P*	0.022	0.001	0.001	0.001	0.001	0.013

Spearman correlation (*R*) and associated *P* values between VFQ score and QUS measures showed statistically significant correlations between the reproducible QUS indices of vitreous echodensity and the patient's subjective assessment of the impact of floaters on vision.

One surprising outcome of this study was that QUS parameters obtained from the posterior region of the vitreous were not reproducible. Since it is quite possible that vitreous opacities in front of the macula could have a greater effect on vision than opacities elsewhere, improvements in ROI definition may be advisable or different ROI shapes may be needed when computing QUS parameters in the premacular region of the vitreous body. Alternatively, it might be important to quantify the histogram (i.e., the underlying probability density function of floaters within a given eye) of the size of the detected floaters, to provide enhanced information.

Future studies should also consider analyzing the variable effect(s) on CS induced by vitreous opacities, particularly smaller ones, at different distances from the retinal surface. Also, the size of vitreous opacities in relation to the size of the pupil may be important with regards to its effect on CS.

Lastly, it may also be of value to incorporate an ultrasound assessment of vitreous movement during head turning or ocular saccades. This is relevant because patients frequently report that head and eye movements cause floaters to enter the optical axis and disturb vision during critical times such as reading and driving. Previous studies[37] have explored the use of ultrasonography to evaluate vitreous mobility as an index of viscosity. Future studies could therefore complement the static structural assessment of vitreous echodensity presented herein with a dynamic assessment of vitreous mobility during ocular saccades. There may be value in correlating QUS measurements as well as mobility measurements with reading speed. It is anticipated that this will provide clinicians with more relevant objective ways to assess the severity of vitreous floaters and select the most appropriate patients for therapy.[19] Such a battery of tests of structure and function might furthermore enable an objective assessment of the efficacy of different proposed floater therapies, such as YAG laser or pharmacologic vitreolysis.[38]

Acknowledgments

The authors thank Jesse Gale, MD, and Amitha Ganti for providing assistance during this study. The authors also thank Christian Chabrier and Cedric Venuat of Quantel Medical for assistance with obtaining the ultrasound video images.

Supported by grants from VMR Consulting, Inc. (Newport Beach, CA, USA), the National Eye Institute of the National Institutes of Health (EY024434), Riverside Research, Research and Engineering Internal Research and Development Fund (New York, NY, USA), and an unrestricted grant to the Department of Ophthalmology of Columbia University from Research to Prevent Blindness (New York, NY, USA).

Disclosure: **J. Mamou**, P; **C.A. Wa**, None; **K.M.P. Yee**, None; **R.H. Silverman**, P; **J.A. Ketterling**, P; **A.A. Sadun**, None; **J. Sebag**, P

References

1. Sebag J. *The Vitreous - Structure, Function, and Pathobiology*. New York: Springer-Verlag; 1989.
2. Sebag J. *Vitreous - in Health and Disease*. New York: Springer; 2014.
3. Sebag J, Balazs EA. Morphology and ultrastructure of human vitreous fibers. *Invest Ophthalmol Vis Sci*. 1989;30:1867–1871.
4. Sebag J. Abnormalities of human vitreous structure in diabetes. *Graefes Arch Clin Exp Ophthalmol*. 1993;231:257–260.
5. Sebag J, Nie S, Reiser K, Charles MA, Yu NT. Raman spectroscopy of human vitreous in proliferative diabetic retinopathy. *Invest Ophthalmol Vis Sci*. 1994;35:2976–2980.
6. Sebag J. Diabetic vitreopathy. *Ophthalmology*. 1996;103:205–206.
7. Gale J, Aiello LP, Sebag J. Diabetic vitreopathy. In: Sebag J, ed. *Vitreous - in Health and Disease*. New York, NY: Springer; 2014:57–80.
8. Gale J, Ikuno Y. Myopic vitreopathy. In: Sebag J, ed. *Vitreous - in Health and Disease*. New York, NY: Springer; 2014:113–130.
9. Huang LC, Yee KMP, Wa CA, Nguyen JN, Sadun AA, Sebag J. Vitreous floaters and vision: current concepts and management paradigms. In: Sebag J, ed. *Vitreous - in Health and Disease*. New York, NY: Springer; 2014:771–788.
10. Balazs EA, Denlinger JL. Aging and human visual function. In: Sekular R, Kline D, Dismukes N, eds. *Aging Changes in the Vitreous*. New York, NY: Alan R. Liss; 1982:45.
11. Hayreh SS, Jonas JB. Posterior vitreous detachment: clinical correlations. *Ophthalmologica*. 2004;218:333–343.
12. Chuo JY, Lee TY, Hollands H, et al. Risk factors for posterior vitreous detachment: a case-control study. *Am J Ophthalmol*. 2006;142:931–937.
13. Sebag J. Age-related differences in the human vitreoretinal interface. *Arch Ophthalmol*. 1991;109:966–971.
14. Sebag J. Anatomy and pathology of the vitreo-retinal interface. *Eye (Lond)*. 1992;6(pt 6):541–552.
15. Murakami K, Jalkh AE, Avila MP, Trempe CL, Schepens CL. Vitreous floaters. *Ophthalmology*. 1983;90:1271–1276.
16. Dorr M, Lesmes LA, Lu ZL, Bex PJ. Rapid and reliable assessment of the contrast sensitivity function on an iPad. *Invest Ophthalmol Vis Sci*. 2013;54:7266–7273.
17. Wagle AM, Lim WY, Yap TP, Neelam K, Au Eong KG. Utility values associated with vitreous floaters. *Am J Ophthalmol*. 2011;152:60–65, e1.
18. Sebag J. Floaters and the quality of life. *Am J Ophthalmol*. 2011;152:3–4.
19. Sebag J, Yee KM, Wa CA, Huang LC, Sadun AA. Vitrectomy for floaters: prospective efficacy analyses and retrospective safety profile. *Retina*. 2014;34:1062–1068.
20. Oshika T, Okamoto C, Samejima T, Tokunaga T, Miyata K. Contrast sensitivity function and ocular higher-order wavefront aberrations in normal human eyes. *Ophthalmology*. 2006;113:1807–1812.
21. Hiraoka T, Okamoto C, Ishii Y, Kakita T, Oshika T. Contrast sensitivity function and ocular higher-order aberrations following overnight orthokeratology. *Invest Ophthalmol Vis Sci*. 2007;48:550–556.
22. Quesnel NM, Lovasik JV, Ferremi C, Boileau M, Ieraci C. Laser in situ keratomileusis for myopia and the contrast sensitivity function. *J Cataract Refract Surg*. 2004;30:1209–1218.
23. Elliott DB, Hurst MA. Simple clinical techniques to evaluate visual function in patients with early cataract. *Optom Vis Sci*. 1990;67:822–825.
24. Rubin GS, Adamsons IA, Stark WJ. Comparison of acuity, contrast sensitivity, and disability glare before and after cataract surgery. *Arch Ophthalmol*. 1993;111:56–61.
25. Leyland M, Zinicola E. Multifocal versus monofocal intraocular lenses in cataract surgery: a systematic review. *Ophthalmology*. 2003;110:1789–1798.
26. Yamauchi T, Tabuchi H, Takase K, Ohsugi H, Ohara Z, Kiuchi Y. Comparison of visual performance of multifocal intraocular lenses with same material monofocal intraocular lenses. *PLoS One*. 2013;8:e68236.
27. Insana MF, Wagner RF, Brown DG. Describing small-scale structure in random media using pulse-echo ultrasound. *J Acoust Soc Am*. 1990;87:179–192.
28. Coleman DJ, Rondeau MJ, Silverman RH, et al. Correlation of microcirculation architecture with ultrasound backscatter parameters of uveal melanoma. *Eur J Ophthalmol*. 1995;5:96–106.
29. Mamou J, Coron A, Oelze ML, et al. Three-dimensional high-frequency backscatter and envelope quantification of cancerous human lymph nodes. *Ultrasound Med Biol*. 2011;37:345–357.
30. Oelze ML, Zachary JF, O'Brien WD Jr. Characterization of tissue microstructure using ultrasonic backscatter: theory and technique for optimization using a Gaussian form Factor. *J Acoust Soc Am*. 2002;112:1202–1211.
31. Lizzi FL, Ostromogilsky M, Feleppa EJ, Rorke MC, Yaremko MM. Relationship of ultrasonic spectral parameters to features of tissue microstructure. *IEEE Trans Ultrason Ferroelectr Freq Contr*. 1986;33:319–329.
32. Mamou J, Oelze ML. *Quantitative Ultrasound in Soft Tissues*. New York, NY: Springer; 2013.
33. Bach M. The Freiburg Visual Acuity test–automatic measurement of visual acuity. *Optom Vis Sci*. 1996;73:49–53.
34. Buhren J, Terzi E, Bach M, Wesemann W, Kohnen T. Measuring contrast sensitivity under different lighting conditions: comparison of three tests. *Optom Vis Sci*. 2006;83:290–298.
35. Dennis RJ, Beer JM, Baldwin JB, Ivan DJ, Lorusso FJ, Thompson WT. Using the Freiburg Acuity and Contrast Test to measure visual performance in USAF personnel after PRK. *Optom Vis Sci*. 2004;81:516–524.
36. Mamou J, Coron A, Hata M, et al. Three-dimensional high-frequency characterization of cancerous lymph nodes. *Ultrasound Med Biol*. 2010;36:361–375.
37. Walton KA, Meyer CH, Harkrider CJ, Cox TA, Toth CA. Age-related changes in vitreous mobility as measured by video B scan ultrasound. *Exp Eye Res*. 2002;74:173–180.
38. Sebag J. Pharmacologic vitreolysis–premise and promise of the first decade [guest editorial]. *Retina*. 2009;29:871–874.

Investigative Ophthalmology & Visual Science